

Magnetic control of electric polarization in the noncentrosymmetric compound (Cu,Ni)B₂O₄N. D. Khanh,^{1,2} N. Abe,² K. Kubo,^{1,2} M. Akaki,³ M. Tokunaga,³ T. Sasaki,⁴ and T. Arima²¹*Department of Physics, Tohoku University, Sendai 980-8577, Japan*²*Department of Advanced Materials Science, The University of Tokyo, Kashiwa 277-8561, Japan*³*Institute for Solid State Physics, The University of Tokyo, Kashiwa 277-8581, Japan*⁴*Institute for Materials Research, Tohoku University, Sendai 980-8577, Japan*

(Received 1 February 2013; revised manuscript received 8 April 2013; published 16 May 2013)

The weak ferromagnetic moment in Ni-doped CuB₂O₄ can be rotated by applying an electric field. While this implies spin-driven ferroelectricity, no direct evidence of electric polarization has been reported to date. Here we report the induction and control of polarization in the borate in the presence of an external magnetic field. Applying a magnetic field along the [110] or $[\bar{1}\bar{1}0]$ axis induces electric polarization along the [001] axis. The polarization is reversed by switching the magnetic-field direction between the [110] and $[\bar{1}\bar{1}0]$ axes. The mechanism by which electric polarization emerges can be well explained in the framework of spin-dependent metal-ligand hybridization.

DOI: 10.1103/PhysRevB.87.184416

PACS number(s): 75.85.+t

Multiferroics is an exotic class of matter that can simultaneously host two or more ferroic orders in the same phase.¹ Among several coupling mechanisms involving different types of ferroicity, the magnetoelectric effect appears in the system where both the time-reversal symmetry T and space inversion symmetry I are broken. Thereby, electric polarization can be manipulated by a magnetic field and vice versa. Interest in this topic has been reinvigorated² by milestone discoveries of large ferroelectric polarization,³ the control of the antiferromagnetic domain by electric fields in thin-film BiFeO₃,⁴ and strong magnetoelectric coupling in TbMnO₃⁵ and TbMn₂O₅.⁶ Since these discoveries, numerous materials possessing cross coupling between magnetism and electricity, with fascinating physics properties, have been explored.^{7,8}

This study investigates the magnetoelectric effect in a noncentrosymmetric compound, namely, Ni-doped copper metaborate, (Cu,Ni)B₂O₄. Unlike other cuprate compounds, this material exhibits a complicated magnetic property^{9,10} as well as unique electro-magneto-optic effects.^{11,12} The magnetization vector can be manipulated up to $\pm 30^\circ$ by an electric field in the canted-antiferromagnetic phase of (Cu,Ni)B₂O₄,¹³ implying a strong correlation between magnetic and electric order. Although symmetry analysis suggests that magnetoelectric coupling occurs in this system, a previous study exploring the structure parameters and dielectric constant showed no clear evidence of electric polarization.¹⁴ Here we report the induction and control of electric polarization along the [001] axis in (Cu,Ni)B₂O₄ under a magnetic field. We attribute the origin of this effect to metal-ligand hybridization.

CuB₂O₄ crystallizes in the space group $I\bar{4}2d$ (point group $\bar{4}2m$), as depicted in Fig. 1. A tetragonal unit cell with lattice parameters $a = 11.84 \text{ \AA}$ and $c = 5.62 \text{ \AA}$ admits 12 formulas.¹⁵ Cu²⁺ ions are located at positions $4d$ and $8b$ (in Wyckoff notation) and are denoted Cu A and Cu B , respectively. The Cu²⁺ ion at the A site is surrounded by a square configuration of four oxygen atoms (local symmetry $\bar{4}$), while that at the B site locates in a strongly distorted octahedron formed by six oxygen atoms (local symmetry 2). No remarkable structural difference exists between pure CuB₂O₄ and Ni-doped samples.¹³

The magnetic property of copper metaborate has been extensively investigated. This material undergoes two successive magnetic phase transitions at $T_N = 21 \text{ K}$ and $T^* = 9 \text{ K}$.^{13,16,17} Above the Néel temperature $T_N = 21 \text{ K}$, CuB₂O₄ exhibits no magnetic order in either Cu A or Cu B . Between 21 and 9 K, the magnetic moments of Cu²⁺ at the A sites exit in a canted-antiferromagnetic state confined to the tetragonal basal plane, while the Cu²⁺ spin moments at B sites remain disordered. The magnetic moments of Cu A are canted approximately 3° from the collinear antiferromagnetic state⁹ due to Dzyaloshinskii-Moriya antisymmetric interactions. Below the second transition temperature $T^* = 9 \text{ K}$, both sites of Cu ions exhibit incommensurate helices with the propagation vector $\mathbf{k} = (0, 0, k_z)$.⁹ A study of magnetization in a perpendicular magnetic field $\mathbf{H} \perp [001]$ revealed an anomaly at a critical field $H_C \sim 1.3 \text{ T}$ at 2 K, which tends to shift toward $H = 0$ as the temperature increases to T^* .¹⁷ This behavior reflects a metamagnetic transition from the incommensurate helical phase to the canted commensurate antiferromagnetic order, induced by the magnetic field. By partially substituting nickel for copper, the magnetization in the low-field regime can be strongly enhanced.^{13,16} However, in the range of the magnetic field where electric polarization is investigated, the partial Ni substitution has no significant effect on the magnetic property and electric polarization.

(Cu,Ni)B₂O₄ single crystals were grown by the flux method.¹⁸ Ni concentration was estimated to be 2.7% by energy dispersive spectroscopy. The crystals were characterized by x-ray-diffraction patterns and Laue photographs. The magnetic properties were determined using a superconducting quantum interference device (MPMS, Quantum Design). The displacement current was acquired using an electrometer (KEITHLEY 6517A) with no poling electric field and integrated to obtain the electric polarization P . To investigate the influence of magnetic-field direction, the sample was rotated around its [001] axis in a superconducting magnet cryostat. Magnetization and polarization were examined in a pulsed magnetic field up to 50 T at several temperatures. The measurements in a pulsed magnetic field are described in detail elsewhere.¹⁹

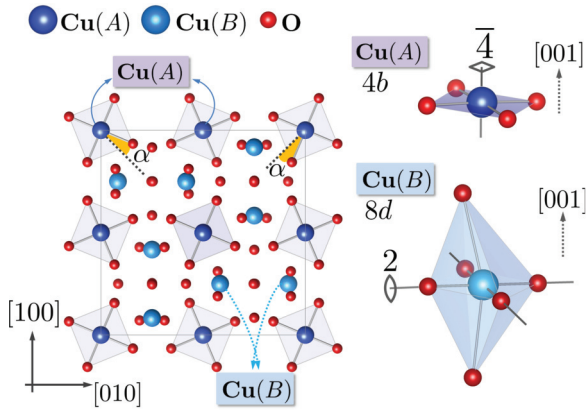


FIG. 1. (Color online) Crystal structure of CuB_2O_4 (boron atoms omitted for simplicity). $\alpha = 22.06^\circ$ defines the orientation of CuO_4 squares with respect to the diagonal line of the tetragonal basal plane.

The magnetic property of $(\text{Cu,Ni})\text{B}_2\text{O}_4$ samples re-examined in this study is consistent with that reported in previous works^{9,16,20} [see Figs. 2(a) and 2(b)]. The results are summarized in a H - T phase diagram in Fig. 2(c). In Fig. 2(d), the electric polarization is plotted as a function of the applied magnetic field and temperature. The application of a magnetic field \mathbf{H} along the $[110]$ direction induces positive polarization $P_{[001]}$ toward the $[001]$ direction. At $T = 4.2$ K, $P_{[001]}$ appears when the magnetic field exceeds a critical value of 1.1 T and gradually increases at higher-field strengths. Similar measurements at different temperatures show that polarization reduces as temperature increases. The critical field that triggers polarization (1.1 T at 4.2 K) also reduces at higher temperature [Fig. 2(d)]. The critical fields for ferroelectric

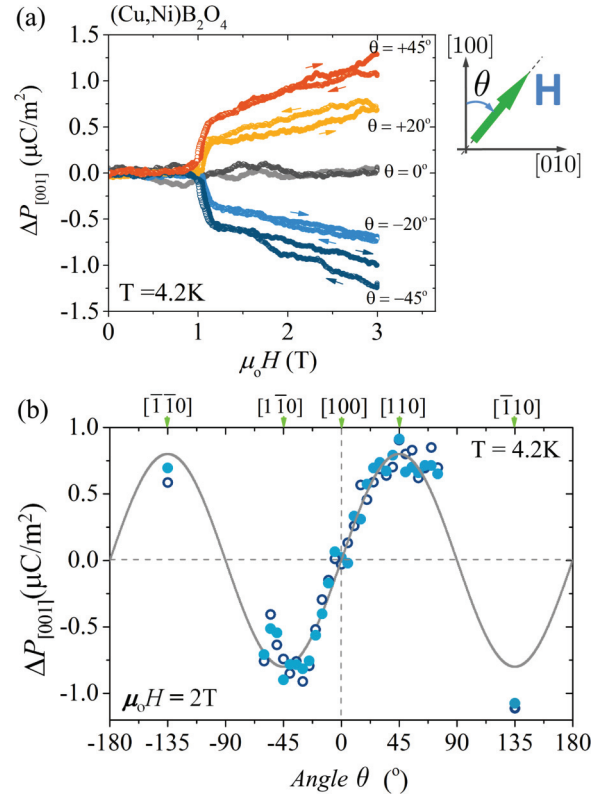


FIG. 3. (Color online) (a) Electric polarization along the $[001]$ axis $P_{[001]}$ of $(\text{Cu,Ni})\text{B}_2\text{O}_4$ as a function of magnetic field \mathbf{H} at $T = 4.2$ K for several magnetic-field directions θ . (b) θ dependence of polarizations $P_{[001]}$ in a magnetic field of 2 T at 4.2 K. Solid (open) symbols present data of polarization $P_{[001]}$ collected during an increase (decrease) of magnetic field. The solid line represents a sinusoidal ($\sin 2\theta$) fit of polarization as a function of angle θ .

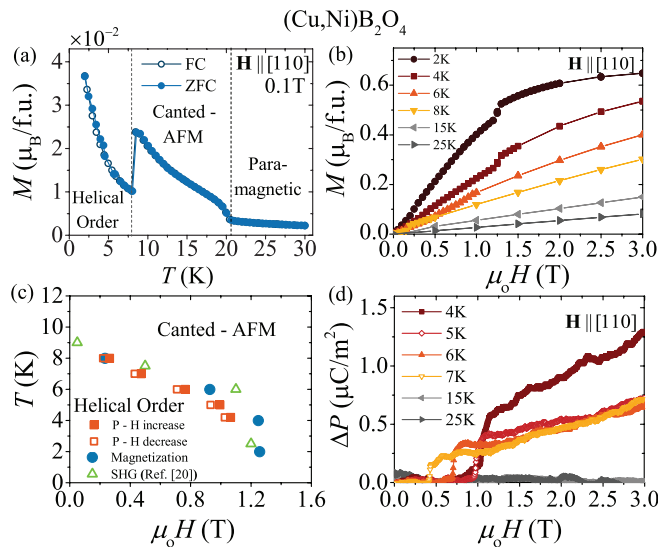


FIG. 2. (Color online) Magnetization as a function of temperature (a) and magnetic field (b). In both cases, magnetic field is applied along the $[110]$ axis. (c) H - T phase diagram at the low-field regime based on measurements of magnetization, polarization, and data of the second-harmonic generation study reproduced from Ref. 20. (d) Magnetic-field dependence of polarization $P_{[001]}$ at several fixed temperatures ($\mathbf{H} \parallel [110]$).

transition are identical to the values H_C , at which the helical phase switches to the canted antiferromagnetic phase. These results imply a mutual correlation between the magnetic order and electric polarization in $(\text{Cu,Ni})\text{B}_2\text{O}_4$. Considering that $P_{[001]}$ appears only when the field exceeds H_C , we infer that the spin arrangement, rather than the magnetic field, is essential for electric polarization.

We next investigate how $P_{[001]}$ evolves under varying magnetic-field direction, implemented by varying the angle θ between the $[100]$ axis and the magnetic-field vector \mathbf{H} . $P_{[001]}$ was measured in magnetic fields up to 3 T at 4.2 K, while θ was swept between 90° ($\mathbf{H} \parallel [010]$) and -90° ($\mathbf{H} \parallel [0\bar{1}0]$). As shown in Fig. 3(a), $P_{[001]}$ gradually increased as the angle θ increased from 0° , reaching an absolute value of $1.2 \mu\text{C}/\text{m}^2$ at $H = 3$ T and $\theta = 45^\circ$ ($\mathbf{H} \parallel [110]$) or -45° ($\mathbf{H} \parallel [1\bar{1}0]$). As the magnetic field was swept from 0 to 3 T, the polarization behaviors in $\mathbf{H} \parallel [110]$ and $\mathbf{H} \parallel [1\bar{1}0]$ were quite similar, but their directions were opposite. $|P_{[001]}|$ slowly decreased to zero as θ approached 90° ($\mathbf{H} \parallel [010]$), consistent with the symmetry argument, which posits that polarization parallel to the $[001]$ axis results from breaking the twofold rotational symmetry around $[100]$ and $[010]$. One should note that the rotating magnetic field affects the magnitude of polarization only and exerts no effect on the critical field of transition to

a ferroelectric state. As shown in Fig. 3(b), $P_{[001]}$ at $H = 2$ T fits the curve $P_{[001]} \propto \sin 2\theta$. Large absolute values of $P_{[001]}$ at $\theta = 135^\circ$ ($\mathbf{H} \parallel [\bar{1}10]$) and -135° ($\mathbf{H} \parallel [1\bar{1}0]$) also support this interpretation, suggesting that $P_{[001]}$ can be reversed by switching the magnetic-field direction between the $[110]$ and $[\bar{1}\bar{1}0]$ axes. Similar behaviors have recently been reported in $\text{Ba}_2\text{CoGe}_2\text{O}_7$,²¹ $\text{Sr}_2\text{CoSi}_2\text{O}_7$,²² and Cu_2OSeO_3 .²³

The continuous change in polarization $P_{[001]}$ as a function of θ cannot be explained by the spin current²⁴ or magnetostriction²⁵ model. Instead, these results can be understood within the framework of spin-dependent metal-ligand hybridization; charge transfer depends on the direction of the spin moment of the transition metal with respect to the metal-ligand bond. The local electric polarization at a transition-metal site i is expressed as

$$\Delta \mathbf{P}_i \propto \sum_j (\mathbf{S}_i \cdot \mathbf{e}_{ij})^2 \mathbf{e}_{ij}, \quad (1)$$

where \mathbf{S}_i denotes the local spin moment of transition metal i and \mathbf{e}_{ij} is the unit vector connecting the metal i and the j th ligand atom. The summation of $\Delta \mathbf{P}_i$ across the whole crystal gives macroscopic electric polarization.^{26,27} Hereafter, we consider that only the copper ions at the A sites contribute to $P_{[001]}$. Around the Cu A sites, two oxygen ions are positioned slightly higher than the Cu atoms, while the other two are lower. Such an atomic arrangement may lead to spin-driven nonzero polarization in this system. From Eq. (1), the local electric polarization in a CuO_4 square is derived as $P \propto \cos 2\varphi$ along the $[001]$ axis, where φ is the angle between the spin moment and the orientation of a metal-ligand bond, as depicted in Fig. 1(b). In this situation, $P_{[001]}$ is largest when the magnetic moments of the transition metal on a magnetic sublattice point toward a ligand ion ($\varphi = 0^\circ$). Conversely, $P_{[001]}$ is predicted to be zero when $\varphi = 45^\circ$. In addition, CuO_4 squares have two different orientations in the crystal, denoted as $A1$ and $A2$ [see Fig. 4(a)]. The contribution of Cu^{2+} in sublattice $A1$ to the

polarization P_{A1} along $[001]$ is proportional to

$$P_{A1} \propto \cos 2 \left(\alpha - \frac{\pi}{4} + \theta - \phi \right), \quad (2)$$

while that in the same direction contributed by Cu^{2+} in sublattice $A2$ is

$$P_{A2} \propto \cos 2 \left(\alpha + \frac{\pi}{4} - \theta - \phi \right). \quad (3)$$

Here ϕ is the canting angle of the Cu^{2+} magnetic moments in the canted-antiferromagnetic state, as shown in Fig. 4(a). The oxygen squares surrounding Cu in the $A1$ and $A2$ sites are oriented $\alpha = 22.06^\circ$ with respect to the diagonal line of the tetragonal basal plane, as in Fig. 1(a).¹⁵ Therefore, the total polarization along the $[001]$ direction can be written as

$$P_{[001]} \propto \sin 2\theta \cos 2(\phi - \alpha). \quad (4)$$

The first component, $\sin 2\theta$, describes the dependence of $P_{[001]}$ on the magnetic-field direction θ , which agrees favorably with the result of Fig. 3(b). The second component, $\cos 2(\phi - \alpha)$, accounts for the influence of magnetic-field strength. A higher magnetic field increases the canting angle ϕ , thereby increasing the polarization to a maximum at $\phi = \alpha$. In this scenario, the magnetic moments of an A -sited Cu reorient toward an oxygen ligand atom, yielding the largest possible electric polarization. As the magnetic field increases, the Cu A magnetic moments of the Cu atom and the ligand sites are again misaligned. Eventually, the polarization should decrease to zero and thereafter reverse its sign. The relationship between magnetic-field direction, magnetic-moment configurations of the A -sited Cu atoms, and respective polarization $P_{[001]}$ is presented in Fig. 4(b).

To test the above inferences, the magnetization \mathbf{M} and polarization $P_{[001]}$ of $(\text{Cu},\text{Ni})\text{B}_2\text{O}_4$ were studied under a pulsed magnetic field \mathbf{H} (up to 50 T) applied along the $[\bar{1}\bar{1}0]$ axis, as shown in Fig. 5. Apart from the metamagnetic transition at $H_C \sim 1.3$ T ($T = 1.6$ K), no magnetization anomalies are observed, indicating that no further magnetic phase transitions occur at higher fields. While the magnetization increases monotonically, the polarization $P_{[001]}$ saturates at $3.5 \mu\text{C}/\text{m}^2$ at around 35 T and appears to decrease under stronger magnetic fields.

The overall relationship between polarization $P_{[001]}$ and magnetic field \mathbf{H} can be quantified by the following simple model. In the canted antiferromagnetic phase, the square lattice of Cu A is described by the Hamiltonian

$$\mathcal{H} = \sum_{i \in A1, j \in A2} J \mathbf{S}_i \cdot \mathbf{S}_j - g \mu_B \sum_{i \in A} \mathbf{S}_i \cdot \mathbf{H}. \quad (5)$$

The first term presents the Heisenberg exchange between nearest-neighbor magnetic moments of Cu A atoms, where J is the antiferromagnetic coupling constant. The second term describes the effect of the external magnetic field \mathbf{H} via the Zeeman interaction. Because the external field exerts a strong influence on the behavior of the system, the antisymmetric Dzyaloshinskii-Moriya interaction term $\mathbf{D}_{\text{DM}} \cdot \sum_{ij} \mathbf{S}_i \times \mathbf{S}_j$ can be neglected. The in-plane exchange interaction parameter J is related to the Néel temperature by $\frac{1}{2} \frac{JnS(S+1)}{3} = k_B T_N$, where n is the number of nearest-neighbor magnetic moments.

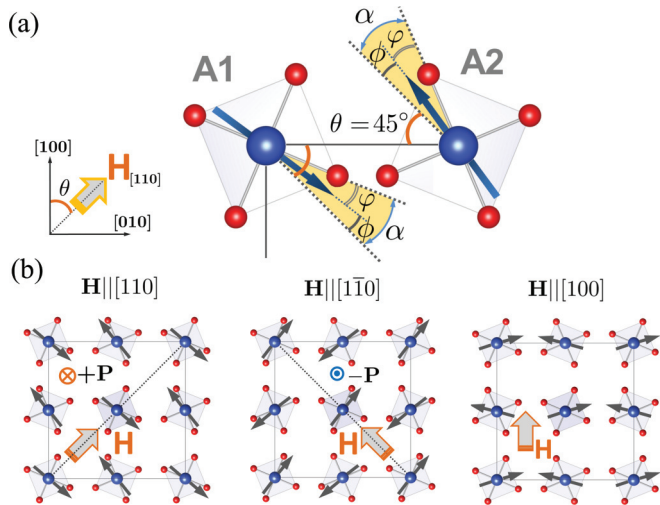


FIG. 4. (Color online) (a) Magnetic moments of Cu^{2+} at $A1$ and $A2$ sublattices in an external magnetic field oriented along the $[110]$ axis ($\theta = 45^\circ$). (b) Schematic expression of Cu^{2+} spin moment (black arrows) configurations at A sites and corresponding polarization $P_{[001]}$ in different directions of the magnetic field.

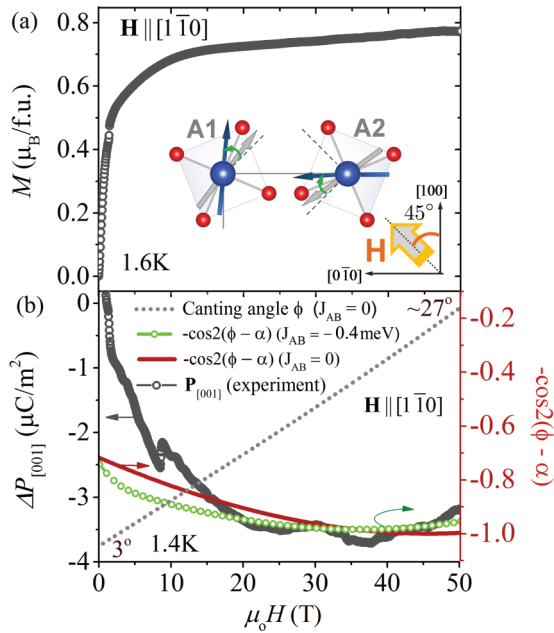


FIG. 5. (Color online) Magnetization (a) and polarization (b) against magnetic field $H \parallel [1\bar{1}0]$ up to 50 T. The dotted line in (b) plots the variation of canting angle ϕ from 0 to approximately 30° estimated from a simple model in Eq. (5) ($J_{AB} = 0$). The solid-dotted and solid lines in (b) exhibit the value of $-\cos 2(\phi - \alpha)$ in the case $J_{AB} = -0.4$ and 0 meV, respectively. The inset in (a) illustrates the variation of magnetic moments at the Cu A site during the increase of applied magnetic field.

For $(\text{Cu,Ni})\text{B}_2\text{O}_4$, $T_N \simeq 21$ K and $n = 4$; thus $J \simeq 3.62$ meV, acceptably close to the value of 3.88 meV obtained from neutron-scattering data.²⁸ Setting $S = 1/2$ and $g \approx 2$, the energy of the system can be written in terms of the canting angle ϕ and magnitude of magnetic field H as

$$\langle \mathcal{H} \rangle = -2J \cos 2\phi - 4\mu_B H \sin \phi. \quad (6)$$

At equilibrium, $\sin \phi = \mu_B H / 2J$; therefore, the dependence of the canting angle ϕ on magnetic field H is $\phi = \arcsin(\mu_B H / 2J)$. The polarization $P_{[001]} \propto \cos 2(\phi - \alpha)$ then becomes

$$P_{[001]} \propto \left(1 - \frac{\mu_B^2 H^2}{2J^2}\right) \cos 2\alpha + \sin 2\alpha \frac{\mu_B H}{J} \sqrt{1 - \frac{\mu_B^2 H^2}{4J^2}}. \quad (7)$$

Figure 5(b) plots the calculated canting angles ϕ and $P_{[001]}$ as a function of magnetic field H , together with the experimental $P_{[001]}$. The polarization $P_{[001]}$ values calculated from Eq. (7) behave similarly to the experimental data up to 50 T. Both increase to a saturated value (at $\phi = \alpha = 22.06^\circ$), then tend to decrease as the applied field exceeds 50 T. However, the calculations based on the square lattice of Cu A do not

completely describe the experimental phenomena. First, while no polarization should exist in the absence of a magnetic field, the calculated $P_{[001]}$ is finite at $H = 0$, which may explain the difference between calculated and experimental $P_{[001]}$ at low field. Nevertheless, at higher fields, where the magnetic moments at the Cu B sites saturate at $\frac{2}{3}\mu_B/\text{f.u.}$, the electric polarization $P_{[001]}$ is mainly driven by the spin moments of Cu A sites, as discussed above. In addition, the measured polarization $P_{[001]}$ saturates at around 35 to 40 T, while the maximum calculated $P_{[001]}$ (P_{max}) is ~ 50 T. This effect may result from magnetic-moment interactions between the A and B sites. To correct for these interactions, an additional term $\sum_{i \in A, j \in B} J_{AB} \mathbf{S}_i \cdot \mathbf{S}_j$ is added to the Hamiltonian in Eq. (5). Here J_{AB} is the exchange interaction constant between nearest-neighbor Cu^{2+} magnetic moments at the A and B sites. Relative to the case $J_{AB} = 0$, the calculated P_{max} shifts toward the lower-field regime when $J_{AB} < 0$, while $J_{AB} > 0$ increases the magnetic field at which P_{max} appears. The experimental and calculated values of saturated $P_{[001]}$ favorably agree when $J_{AB} \sim -0.4$ meV,²⁹ corresponding to a ferromagnetic exchange between the magnetic moments at the A and B sites, although this result requires further investigation.

In conclusion, we conducted experiments to investigate the magnetoelectric effect in the $(\text{Cu,Ni})\text{B}_2\text{O}_4$ system. The results indicate that electric polarization can be generated and controlled in this material by applying a magnetic field. More specifically, the material can be polarized along the [001] direction by applying the field parallel to the diagonal line of the tetragonal basal plane. Polarization was found to correspond to a metamagnetic transition from a helical to a canted antiferromagnetic state. In addition, rotating the magnetic field in the tetragonal plane caused the polarization to vary sinusoidally as 2θ (where θ is the angle between the magnetic-field vector and the [100] axis). In this way, the polarization can be reversed by switching the magnetic-field orientation between the [110] and $[1\bar{1}0]$ axes. These behaviors suggest that electric polarization in $(\text{Cu,Ni})\text{B}_2\text{O}_4$ can be reasonably described by a metal-ligand hybridization model derived from spin-orbit interactions.

ACKNOWLEDGMENTS

The authors acknowledge enlightening discussions with Y. Nii. This work was partly supported by a Grant-in-Aid (Grant No. 24244045) from the Ministry of Education, Culture, Sports, Science, and Technology, Japan, and by the Mitsubishi foundation. The magnetization and magnetoelectric effect in a pulsed magnetic field were measured at the Institute for Solid State Physics, University of Tokyo, Japan. The magnetic-field induced electric polarization in a quasistatic magnetic field was investigated at the High Field Laboratory for Superconducting Materials, Institute for Materials Research, Tohoku University, Japan.

¹For example, see Y. Tokura, *Science* **312**, 1481 (2006); N. Mazur and J. Scott, *Nature (London)* **442**, 759 (2006); R. Ramesh and N. A. Spaldin, *Nat. Mater.* **6**, 21 (2007).

²M. Fiebig, *J. Phys. D* **38**, R123 (2005).

³J. Wang, J. B. Neaton, H. Zheng, V. Nagarajan, S. B. Ogale, B. Liu, D. Viehland, V. Vaithyanathan, D. G. Schlom, U. V. Waghmare, N. A. Spaldin, K. M. Rabe, M. Wuttig, and R. Ramesh, *Science* **299**, 1719 (2003).

- ⁴T. Zhao, A. Scholl, F. Zavaliche, K. Lee, M. Barry, A. Doran, M. P. Cruz, Y. H. Chu, C. Ederer, N. A. Spaldin, R. R. Das, D. M. Kim, S. H. Baek, C. B. Eom, and R. Ramesh, *Nat. Mater.* **5**, 823 (2006).
- ⁵T. Kimura, T. Goto, H. Shintani, K. Ishizaka, T. Arima, and Y. Tokura, *Nature (London)* **426**, 55 (2003).
- ⁶N. Hur, S. Park, P. A. Sharma, J. S. Ahn, S. Guha, and S. W. Cheong, *Nature (London)* **429**, 392 (2004).
- ⁷T. Arima, *J. Phys. Soc. Jpn.* **80**, 052001 (2011).
- ⁸D. Khomskii, *Physics* **2**, 20 (2009).
- ⁹M. Boehm, B. Roessli, J. Schefer, A. Wills, B. Ouladdiaf, E. Lelievre-Berna, U. Staub, and G. A. Petrakovskii, *Phys. Rev. B* **68**, 024405 (2003).
- ¹⁰G. Petrakovskii, D. Velikanov, A. Vorotynov, A. Balaev, K. Sablina, A. Amato, B. Roessli, J. Schefer, and U. Staub, *J. Magn. Magn. Mater.* **205**, 105 (1999).
- ¹¹M. Saito, K. Taniguchi, and T. Arima, *J. Phys. Soc. Jpn.* **77**, 013705 (2008).
- ¹²M. Saito, K. Ishikawa, K. Taniguchi, and T. Arima, *Phys. Rev. Lett.* **101**, 117402 (2008).
- ¹³M. Saito, K. Ishikawa, S. Konno, K. Taniguchi, and T. Arima, *Nat. Mater.* **8**, 634 (2009).
- ¹⁴G. Nénert, L. N. Bezmaternykh, A. N. Vasiliev, and T. T. M. Palstra, *Phys. Rev. B* **76**, 144401 (2007).
- ¹⁵M. Martinez-Ripoll, S. Carrera-Martinez, and S. Garcia-Blanco, *Acta Crystallogr. B* **27**, 677 (1971).
- ¹⁶G. A. Petrakovskii, L. V. Udod, K. A. Sablina, A. I. Pankrats, S. N. Martynov, D. A. Velikanov, R. Szymczak, M. Baran, A. F. Bovina, and G. V. Bondarenko, *Phys. Met. Metallogr.* **99**, S53 (2005).
- ¹⁷G. A. Petrakovskii, A. I. Pankrats, M. A. Popov, A. D. Balaev, D. A. Velikanov, A. M. Vorotynov, K. A. Sablina, B. Roessli, J. Schefer, A. Amato, U. Staub, M. Boehm, and B. Ouladdiaf, *Low Temp. Phys.* **28**, 606 (2002).
- ¹⁸G. A. Petrakovskii, K. A. Sablina, D. A. Velikanov, A. M. Vorotynov, N. V. Volkov, and A. F. Bovina, *Crystallogr. Rep.* **45**, 853 (2000).
- ¹⁹M. Tokunaga, *Front. Phys.* **7**, 386 (2012).
- ²⁰R. V. Pisarev, I. Sanger, G. A. Petrakovskii, and M. Fiebig, *Phys. Rev. Lett.* **93**, 037204 (2004).
- ²¹H. Murakawa, Y. Onose, S. Miyahara, N. Furukawa, and Y. Tokura, *Phys. Rev. Lett.* **105**, 137202 (2010).
- ²²M. Akaki, H. Iwamoto, T. Kihara, M. Tokunaga, and H. Kuwahara, *Phys. Rev. B* **86**, 060413(R) (2012).
- ²³M. Belesi, I. Rousochatzakis, M. Abid, U. K. Robler, H. Berger, and J. Ph. Ansermet, *Phys. Rev. B* **85**, 224413 (2012).
- ²⁴H. Katsura, N. Nagaosa, and A. V. Balatsky, *Phys. Rev. Lett.* **95**, 057205 (2005).
- ²⁵I. A. Sergienko and E. Dagotto, *Phys. Rev. B* **73**, 094434 (2006).
- ²⁶T. Arima, *J. Phys. Soc. Jpn.* **76**, 073702 (2007).
- ²⁷C. Jia, S. Onoda, N. Nagaosa, and J. H. Han, *Phys. Rev. B* **76**, 144424 (2007).
- ²⁸M. Boehm, S. Martynov, B. Roessli, G. Petrakovskii, and J. Kulda, *J. Magn. Magn. Mater.* **250**, 313 (2002).
- ²⁹The dependence of canting angle ϕ to the magnetic field in the case of considering the interaction between magnetic moments at the A sites and B sites can be estimated by solving the Hamiltonian in Eq. (5) with the additional term $\sum_{i \in A, j \in B} J_{AB} \mathbf{S}_i \cdot \mathbf{S}_j$, which leads to the equation $2J \sin \phi = \mu_B H - 2J_{AB} \langle S_B \rangle$, in which the evolution of magnetic moments at the B sites can be evaluated via Brillouin function as $\langle S_B \rangle = \frac{1}{2} \tanh\left(\frac{\mu_B H - J_{AB} \sin \phi}{k_B T}\right)$. Thereby, the influence of exchange constant J_{AB} to the polarization $P_{[001]} \sim \cos 2(\phi - \alpha)$ in an applied magnetic field H can be obtained as in the main text.